지구물리 제 4권 제 1호, p. 35-46, (2001년 3월)

Crustal Structure under the Taejon(TJN) Station by Receiver Function Methods

Hyunjae Yoo and Kiehwa Lee

School of Earth and Environmental Sciences, Seoul National University

ABSTRACT

Inversions of receiver functions from teleseismic waves recorded at Taejon(TJN) seismic station located in the central region of the Korean peninsula yield 1-D velocity structures that are compatible with the observed waveforms. To investigate the reliability of the technique and the initial model dependence, a series of inversions with three initial model groups of 72 models was performed. The 43 models among 72 ones agree reasonably well with the observed data. The structure derived from receiver functions obtained at TJN station is relatively simple, consisting of an approximately 30 to 32.5 km thick crust having no significant discontinuity or positive velocity gradient. All models have relatively sharp crust-mantle boundaries with a change in P-wave velocity from about 6.5 km/s to approximately 7.8 km/s over a depth range of 2 to 3 km. The earth models can be roughly divided into two groups that differ mostly in the mid-crust. The first group of earth models contains a slight low-velocity zone in the mid-crust, while the other group has nearly constant velocities through the mid-to-lower crust. It is difficult to distinguish between the two velocity structures on the basis of receiver function waveforms alone. To resolve this problem, other a priori information is required.

Key words: Receiver function, crustal structure, low-velocity zone, Korean peninsula

Hyunhae Yoo and Kiehwa Lee, 2001, Crustal Structure under the Taejon(TJN) Station by Rrceiver Function Methods. Journal of the Korean Geophysical Society, v. 4, n. 1, p. 35-46

요약: 한반도 중부에 위치한 대전 지진관측소(TJN) 하부의 세부 지각구조를 밝혀내기 위하여 수신함수를 이용한 선형화된 역산(linearized inversion) 방법을 적용하였다. 본 방법의 비단일해(nonuniqueness)와 초기 모델 의존성의 문제를 해결하기 위해 근사 초기 속도 모델로부터 72 개의 서로 다른 초기 모델을 구하여 역산을 수행한 후 결과모델들의 평균 속도 모델을 제시하는 방법을 사용하였다. 역산 결과 총 72 개의 모델 중 뚜렷한 지각-맨틀 경계를 보이는 43 개의 모델만이 조건에 만족하는 결과를 나타내었다. 모든 모델에서 속도 구조는 전체적으로 깊이에 따라 속도의 불연속면이나 급격한 증가 없이 연속적인 변화를 하며, 모호면의 깊이는 30 ~ 32.5 km의 범위로 나타났다. 평균적인 하부 지각의 속도는 6.5 km/s, 상부 맨틀의 속도는 7.8 km/s로 뚜렷한 속도 변화를 보였다. 결과 모델 군은 중부지각(mid-crust)에서의 속도를 기준으로 약한 저속도층을 나타내는 군과 상대적으로 일정한 속도를 가지는 군으로 구분되었다. 단지 지진파형의 비교만으로 두 모델군 중 합당한 모델군의 선택은 불가능하였다. 따라서 수신 함수를 이용하여 연구 지역의 신뢰할 만한 지각 구조를 구하기 위해서는 그 지역에 대한 지질학적, 지구물리학적 추가정보와의 동반 해석이 요구된다.

주요어: 수신 함수, 지각 구조, 저속도층, 한반도

(Hyunjae Yoo and Kiehwa Lee, School of Earth and Environmental Sciences, Seoul National University, Shillim-Dong, Kwanak-Gu, Seoul, 151-742, Korea. email: hjyoo5@snu.ac.kr and kihwalee@plaza.snu.ac.kr)

1. Introduction

Accurate information about crustal velocity structure is necessary for a variety of purposes, such as the determination of earthquake hypocenters, the resonable understanding of seismicity, the proper analysis of seismic hazard, and the interpretation of geophysical characteristics of the area concerned. In the Korean peninsula, the crustal velocity structure was studied by some researchers using various methods(Lee, 1979; Kim and Kim, 1983; Kim and Jung, 1985; Kim, 1995). Lee(1979) presented a one-layered crustal model with average crustal P-wave velocity of 5.8 km/s, Pn velocity of 7.7 km/s, and the crustal thickness of 35 km. He observed that it was not clear whether the crust was single-layered or multi-layered. Although Kim and Kim(1983) suggested a two layerd crustal model, and Kim and Jung(1985) and Kim(1995) presented a three-layered crustal model with a thin top layer of low velocity, they didn't provide seismic phases indicating discontinuities in the crust as a clear evidence on the layering of the crust of the Korean peninsula.

Among various methods a particularly simple technique for obtaining crustal velocity information is teleseismic P wave receiver function modeling (Langston, 1977; Langston, 1979; Owens *et al.*, 1984; Owen *et al.*, 1987; Ammon and Zandt, 1993). This technique provides detailed seismic velocity information for the crust and upper mantle in a localized region containing the station site. This research presents the modeling of observed receiver functions recorded at the TJN station operated by the KIGAM(Korea Institute of Geology, Mining & Materials). The station is located at Taejon(36.381N, 127.362E) area belonged to the Ogcheon system of regionally metamorphosed sedimentary rocks and intruded dykes. The station equipped with a STS-2, broadband three-components(Z, N, E) seismic sensor. Teleseismic broad band data recorded at the TJN station are used to obtain the receiver functions by the source equalization method(Langston, 1979). The receiver functions are used to model the detailed structure of the crust and upper mantle beneath the recording site by the inversion method of Ammon *et al.*(1990).

2. Method

2.1. Receiver Function

Teleseismic P wave incident from mantle upon crust contains information related to the source mechanism, near-source structure, propagation effects through the mantle. It interacts with fine crustal structure generating Ps conversion and many crustal reverberation phases. If the source and lower mantle propagation effects can be eliminated, detailed modeling of the first tens of seconds of the waveform provides constraints on the local velocity structure beneath the receiver.

The receiver function is defined as the time signal generated in the crust beneath the station due to a plane P wave incident from the mantle. It contains all crustal reverberations and multiple conversions which arrive in the coda of the direct P wave. Figure 1 shows the schematic of the effects of local structure on teleseismic P waves and synthetic radial receiver function for simple crust. In Figure 1, multiples are

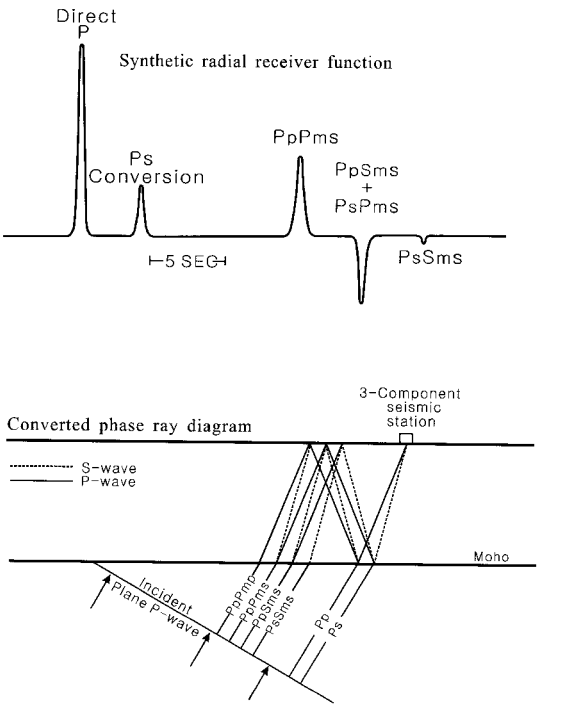

Fig. 1. Schematic ray diagram and synthetic receiver function for simple crust(After Owen, 1984).

labeled using the notation of Bath and Stefanson (1966). Except for the first arrival, upper case letters denote up-going travel paths, lower case letters denote down-going travel paths, and m indicates reflection from the Moho. By modeling this receiver function accruing from the teleseismic P waves, the crustal structure beneath a station can be elucidated in some detail.

2.2. Source Equalization Procedure

The theoretical ground displacement produced by a plane P wave impinging at the base of a stack of horizontal or dipping interfaces is the composite of the interaction of several effects: 1) the form of the impinging wavelet, 2) the earth structure beneath the recording station, and 3) the recording instrument response. Mathematically, the ground motion is represented by the convolution of the above effects:

$$D_V(t) = S(t) * E_V(t) * I(t) \quad (1)$$

$$D_R(t) = S(t) * E_R(t) * I(t) \quad (2)$$

$$D_T(t) = S(t) * E_T(t) * I(t) \quad (3)$$

where the subscripts V, R, and T imply vertical, radial, and tangential, respectively; D(t) represents ground motion; S(t), the apparent source time function, represents the form of the wave impinging beneath the structure; E(t), the impulse response of local earth structure, or the receiver function; I(t), the recording instrument response; and asterisk designates convolution. Langston's(1979) source equalization scheme assumes that

$$E_V(t) \sim \delta(t) \quad (4)$$

where $\delta(t)$ is the Dirac delta function. There obviously are errors in this assumption. However, these errors are tolerable, even for large velocity contrasts, when weighed against the many advantages it provides. From (4) and (1), we see now that

$$D_V(t) \sim I(t) * S(t) \quad (5)$$

Thus, $D_V(t)$ contains exactly the factors that we wish to remove from our observed seismograms. Assuming that instrument responses are matched between components, $E_R(t)$ and $E_T(t)$ may be found by deconvolving $I(t) * S(t)$ from $D_R(t)$ and $D_T(t)$. To stabilize the deconvolution, the method involves the introduction of a minimum allowable value in the denominator(Helmberger and Wiggins, 1971; Clayton and Wiggins, 1976). One further step, in order to avoid high frequency noise introduced by the spectral division, is to smooth the result with a gaussian pulse. The final form of the deconvolution is as follows

$$E_R(\omega) = \frac{D_R(\omega)\overline{D_V(\omega)}}{\Omega(\omega)} G(\omega)$$
$$E_T(\omega) = \frac{D_T(\omega)\overline{D_V(\omega)}}{\Omega(\omega)} G(\omega) \quad (6)$$

where, $\Omega(\omega) = \max\{D_V(\omega)\overline{D_V}(\omega), c\max[D_V(\omega)\overline{D_V}(\omega)]\}$ and $G(\omega) = -\omega^2/(4a^2)$. The value of c ($c \leq 1.0$) is termed the water-level parameter(Clayton and Wiggins, 1976) and controls the minimum value of $\Omega(\omega)$, and $\overline{D_v}$ indicates complex conjugate of D_v. The value of a controls the width of the Gaussian filter. Clayton and Wiggins(1976) demonstrates that the value of c controls the trade-off between arrival time ($c=0.0$) and amplitude ($c=1.0$) resolution. Noise from both spectral troughs in the vertical component and high-frequency noise may increase as c decreases. High frequency noise may be reduced in some cases by varying the width of the Gaussian filter a - the value of a limits the frequency content of the deconvolution result. However, this generally smooths some adjacent peaks together in the result and could reduce our ability to identify distinct phases. Therefore, the appropriate values of c and a are chosen subjectively and empirically so that the deconvolution results have high S/N ratio and mostly represent the apparent receiver structure. In this research, we used the water-level parameter of 0.001 and the Gaussian width parameter of 2.5.

2.3. Inversion Procedure

We used a linearized inversion scheme of Ammon

et al.(1990) employing the "jumping" algorithm of Parker(Constable *et al.*, 1987) to invert receiver functions. We have to solve

$$\begin{bmatrix} D \\ \sigma\Delta \end{bmatrix} m \approx \begin{bmatrix} r \\ 0 \end{bmatrix} + \begin{bmatrix} Dm_0 \\ 0 \end{bmatrix} \quad (7)$$

where, m is S-wave velocity vector(m_0 is the initial model), r is residual vector, σ is smoothness factor that controls the trade-off between data fit and model roughness and Δ is a differencing matrix that computes the model roughness. The matrix D has dimensions $N \times M$ and is often referred to as the data kernel. The element of D is demonstrating the sensitivity of the time sample in the synthetic receiver function to small changes in the layer velocity of m_0.

We implement a smoothness constraint in our inversions by minimizing a model roughness norm (Constable *et al.*, 1987). Minimizing the roughness of the model can trade-off with fitting more details in the waveform. The approach does not eliminate first-order discontinuities in the model but produces an overall smoother velocity profile. To implement the smoothness constraint, we minimize the second difference of the model for all examples shown in this work. The adjustable parameter σ controls the trade-off between fitting the waveform and smoothness of the model. We invert for velocity structures consisting exclusively of horizontal layers with fixed thicknesses. To reduce computational costs, layer thicknesses are kept between 2 and 3 km. Although the number of layers is large(typically 20-30), the smoothness constraint limits the number of free parameters in an inversion. We adjust the P-velocity assuming a Poisson solid.

3. Data Analysis

Teleseismic broadband data recorded at the TJN station from the three azimuths corresponding to events in Indonesia(south), the southwest Pacific (southeast), and Alaska(northeast) are used to obtain the receiver functions(Figure 2). Table 1 presents

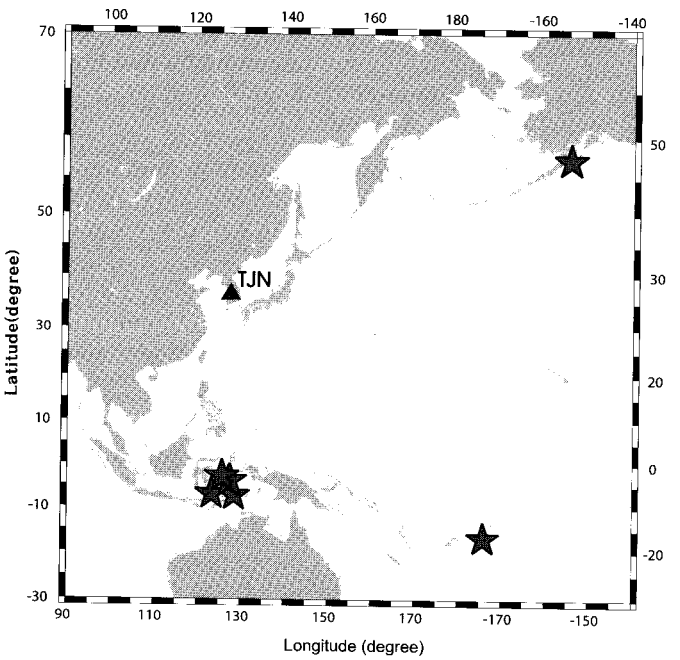

Fig. 2. Location map of six earthquake events used in this study and TJN seismic station. Source parameters of each event are described in Table 1.

Table 1. Source parameters for events recorded at Taejon(TJN) station.

ID	Date (y/m/d)	Origin time (h:m:s)	Latitude (°N)	Longitude (°E)	Depth (km)	Magnitude	Back-Azimuth (°N)	Distance (°)	Ray Parameter (sec/km)	Location
*01	00/03/03	22:09:13.8	-7.320	128.490	141.9	6.4	178.4	43.50	0.073	Indonesia
*02	00/08/07	14:33:55.91	-7.020	123.357	648.5	6.5	185.5	43.30	0.073	Indonesia
*03	00/08/28a	19:29:25.0	-4.140	127.250	33.0	6.5	180.2	40.30	0.075	Indonesia
*04	00/08/28b	15:05:47.9	-4.018	127.520	16.0	6.8	179.8	40.20	0.075	Indonesia
05	00/01/08	16:47:20.58	-16.930	-174.250	183.4	6.5	123.0	76.47	0.051	West-Pacific
06	99/02/06	23:12:33.92	57.410	-154.490	66.0	6.8	40.8	54.10	0.066	Alaska

*Events used to compute receiver function stacks.

the source parameters for six events. Unfortunately, the azimuthal coverage of this data set is not sufficient for estimating three-dimensional velocity structure but we could roughly get the idea of lateral velocity variations.

From the three-component seismograms for each event, radial and tangential component are deconvloved by vertical component using source equalization method(Langston, 1979) to obtain the receiver functions. The water-level for the stable deconvolution is set to 0.001, and the Gaussian width parameter is given as 2.5 which corresponds to filtering out frequency range higher than about 0.6 Hz. Figure 3 presents the source-equalized, stacked (south) or single(southeast, northeast) receiver functions for the three quadrants. For both southeast and northeast directions, because there is only one earthquake event appropriate for receiver function analysis, we could not get stacked receiver functions for each direction. The variation of the lithospheric response as a function of azimuth is somewhat significant, with the south and northeast producing relatively simple radial and tangential receiver functions than the southeast. The south radial receiver function is extremely simple with the direct P arrival followed by only two significant secondary arrivals. The tangential receiver function is for the most part small relative to the radial receiver function arrivals. The southeast radial receiver function is very complicated with numerous secondary arrivals and very little decay in the overall amplitude of the ground motion in the 25 sec following the arrival of the direct P wave. The northeast receiver function is similar to that of the south in the arrival time of two significant secondary arrivals and the duration of ground motion.

The azimuthal variation is in part due to the different incidence angles corresponding to the different azimuths. Events used to construct the south stacked receiver function cluster in the epicentral range of 41° which corresponds to incidence angles at the base of the crust of approximately 34°. The epicentral distances of events used to obtain the southeast and northeast receiver function are 76° and 54°, corresponding to an incidence angle of about 23° and 30°, respectively. Ammon(1991) pointed out that the incidence angle is an important factor in the generation of shear-wave conversions at near-horizontal interfaces. Most previous receiver function studies normalized the receiver functions to unit amplitude, ignoring the variation in the conversion coefficient with incidence angle and neglecting information contained in the amplitude of direct P arrival. The frequency response of the TJN instrument allows us to examine the scattering over a wide frequency band. We varied the width

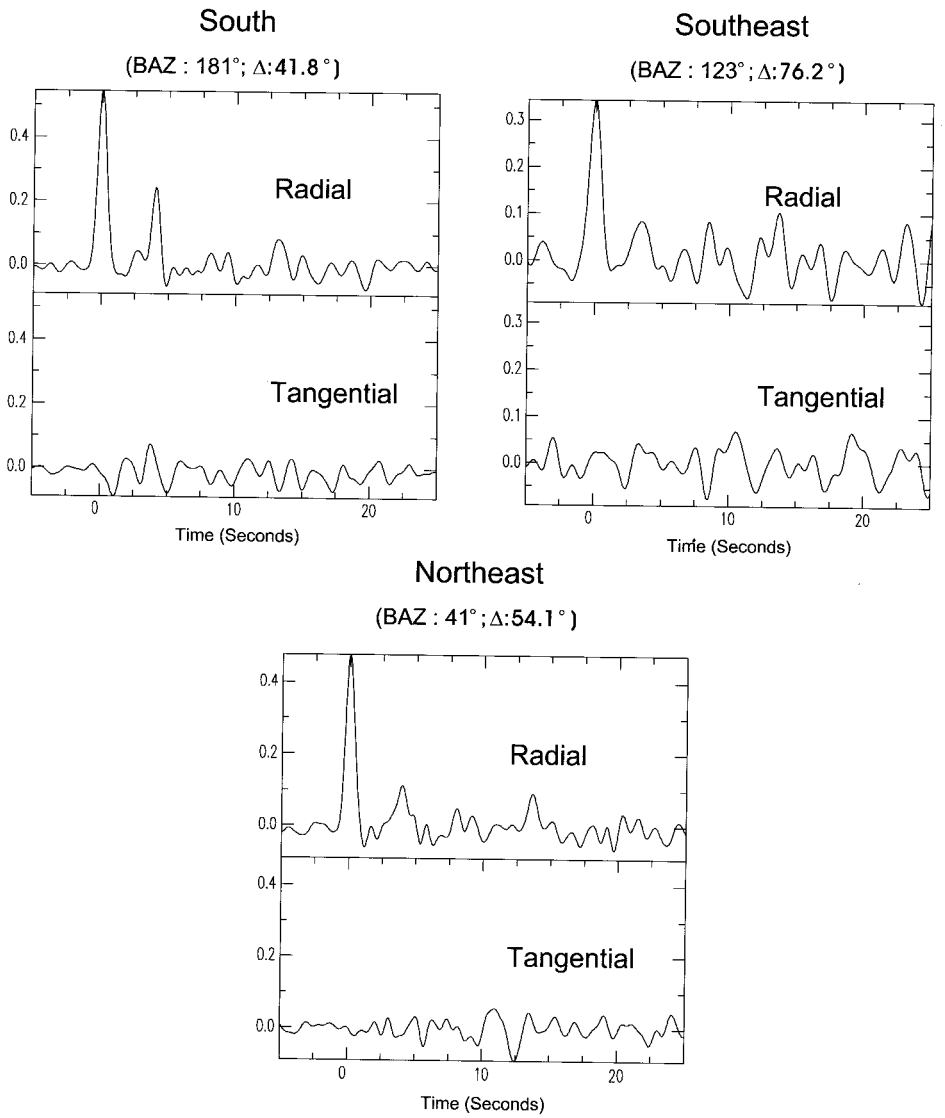

Fig. 3. TJN receiver functions for the three quadrants. Zero time in this and all subsequent figures corresponds to the direct P-wave arrival.

of the Gaussian filter used in the deconvolutions to produce lower frequency receiver functions. Figure 4 presents normalized, radial and tangential receiver functions from the three azimuths filtered with a Gaussian function described by

$$G(\omega) = \exp\left(\frac{-\omega^2}{4\,a^2}\right) \qquad (8)$$

with the Gaussian width fact, a, equal to 0.75, effectively attenuating frequencies above 0.25 Hertz. Assuming a typical shear-wave velocity of 3.5 km/sec these receiver functions are dominated by wavelengths greater than about 14 km. Although not identical, at these frequencies the receiver functions from the different azimuths begin to nearly resemble one another and the south and northeast radial ground motions are significantly larger than the corresponding tangential motions. Therefore, we guess that the gross velocity structures under these three azimuthal direction are almost same and that relatively small

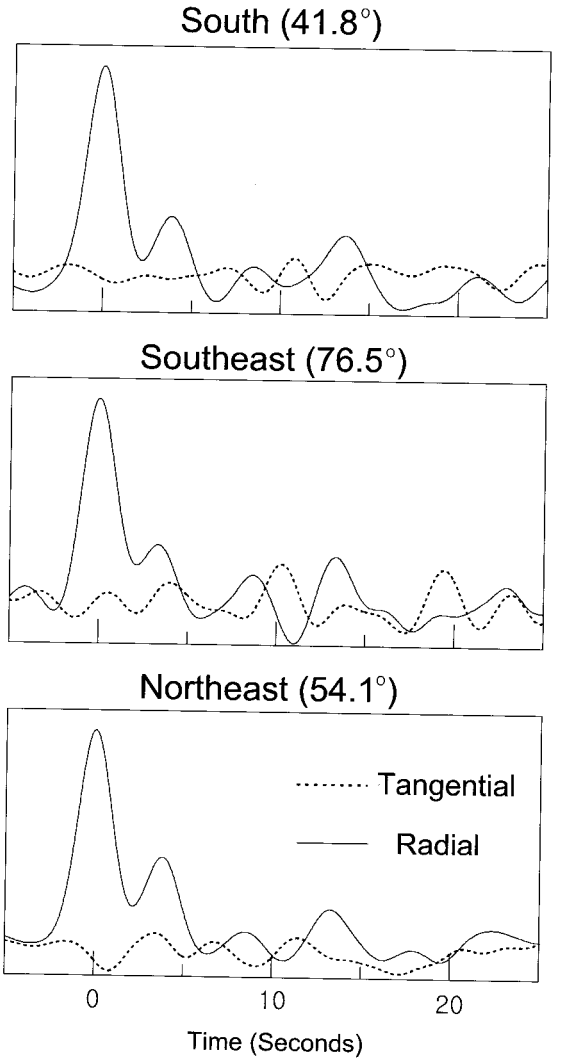

Fig. 4. Low-frequency TJN receiver functions. The azimuth for each receiver function is presented to the top of each normalized waveform, and the distance to the events is indicated to the right of the azimuth.

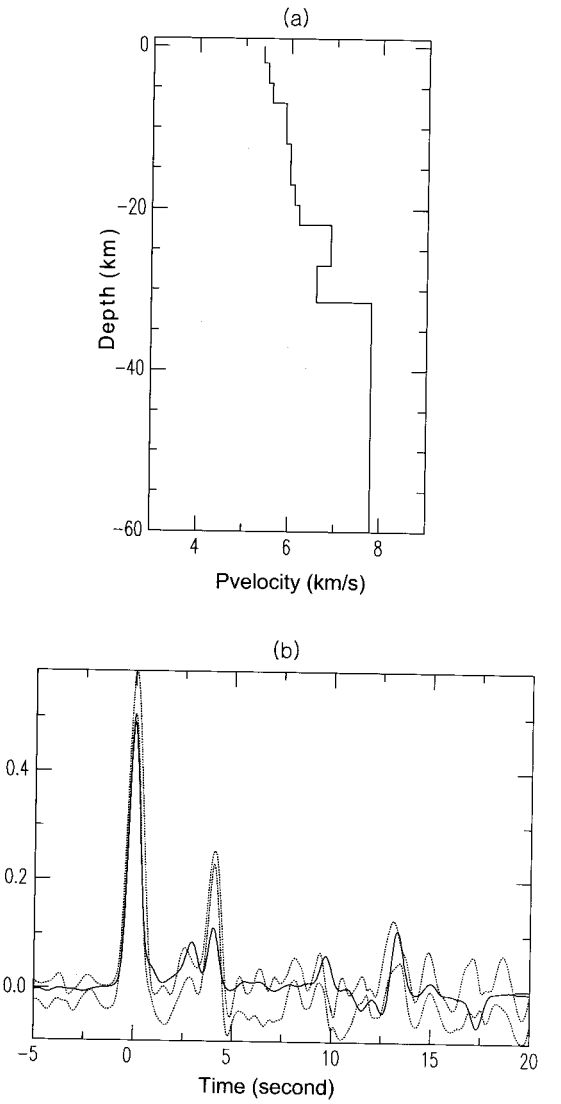

Fig. 5. (a) Initial velocity model used in the inversion of the south radial receiver function. (b) Comparison of the receiver function(solid line) corresponding to the initial model and the standard deviation bounds(dotted line) of the stacked south radial receiver function.

lateral heterogeneity, which is common, is present. However, we can do little to evaluate the details of such lateral velocity variations in this study due to lack of data covering sufficient azimuthal range.

4. Results and Discussions

The sufficient data for stacking and the simplicity of the stacked receiver functions of the south direction enables us to estimate an average vertical crustal structure of south of TJN by modeling the south radial receiver function. The inversion of the receiver function is performed iteratively in the time domain using standard least-squares techniques(Ammon *et al.*, 1990). All geophysical inverse problems are nonunique and most are initial model dependent.

The modest computational demands of receiver function inversions allow us to explicitly examine the initial model dependence and nonuniqueness for this problem.

We constructed an initial velocity model(reference model) for the inversions using the result of forward modeling(Figure 5). To investigate the uniqueness of the technique and the initial model dependence, we performed a series of inversions with three initial model groups. The initial model for each waveform inversion is a perturbed version of the model shown in Figure 5a. To generate the initial velocity models for the inversions, we add perturbation vectors to the reference model. Table 2 summarizes the maximum perturbation amplitudes added to the reference model to assemble the initial models used for this study. Figure 6 displays 3 groups of 24 initial models with different perturbations schemes. Ammon *et al.*(1990) pointed out that this method of generating the initial models can produce a family of initial models which are significantly different from each other but related to the initial unperturbed starting model.

In order to estimate an appropriate value of the smoothness trade-off parameter σ, we inverted the waveform with 12 distinct σ values ranging from 0 to 0.55. Figure 7 quantifies the trade-off between smoothness and waveform fit. Based on the analysis of Figure 7, we chose a smoothness parameter of 0.1 to generate the smoothest model which adequately fits the data. For $\sigma = 0.1$ the RMS residual is 0.018 which is close to the RMS variation of 0.015 for the noise in the 25 sec of the stack preceding the signal.

A total of 72 inversions of the waveform were performed. Of the 72 inversion results, 43 models

Table 2. Construction of the initial models.

	Maximum Cubic Perturbation, Km/s	Variance of Random Perturbation, % of cubic perturbation	Number of Models	Interfaces Shifted, yes/no
Group 01	0.5	20	24	no
Group 02	1.0	20	24	no
Group 03	0.5	20	24	yes

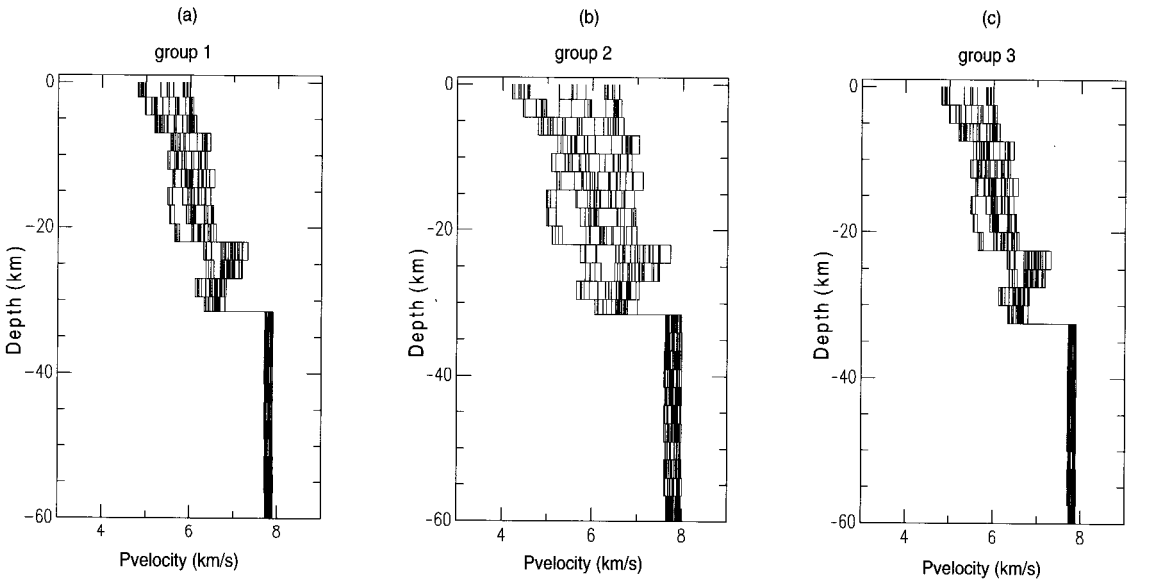

Fig. 6. Three groups of the initial models used in the waveform inversion. Each initial model is calculated by adding three perturbation vectors onto the reference model of Figure 5a. (a) Models generated by adding a cubic perturbation of 0.5 km/s and a random component with a variance equal to 20 % of the cubic perturbation. (b) Models generated by adding a cubic perturbation of 0.75 km/s and a random component with a variance equal to 20 % of the cubic perturbation. (c) Models generated like (a) except for layer shift.

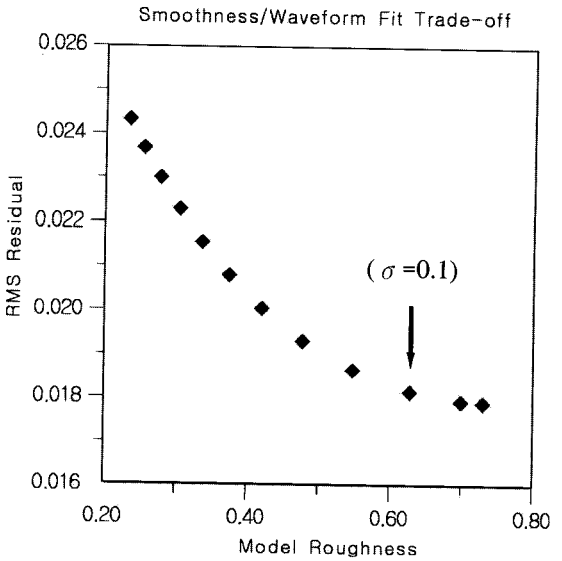

Fig. 7. Smoothness/waveform fit trade-off for the suite of 12 inversions of the TJN receiver function with varying values of the smoothness parameter. The arrow indicates the residual and smoothness of the model resulting with a smoothness parameter value of 0.1, used in the remaining inversions of the waveform.

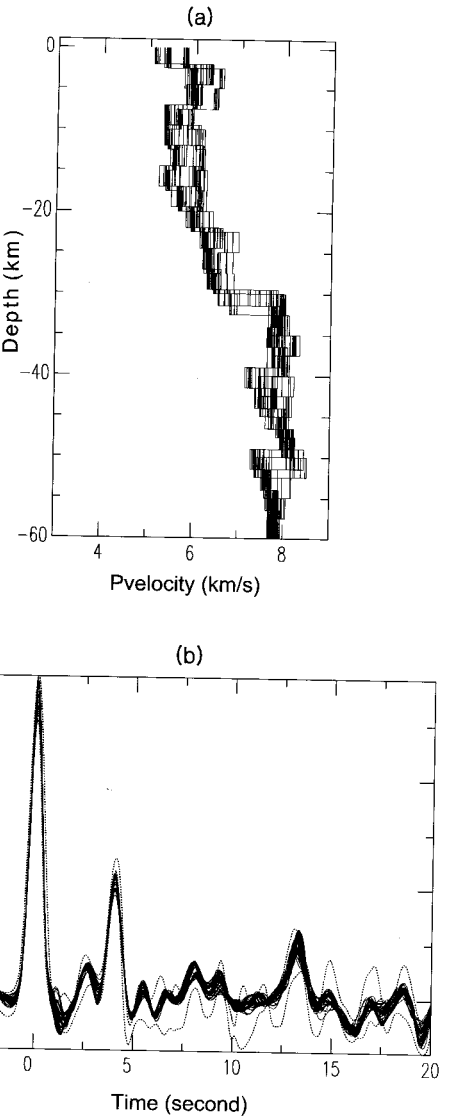

Fig. 8. (a) Forty-three acceptable velocity structures resulting from 72 inversions of the TJN south receiver function. Note the large range in velocity acceptable throughout the middle crust and sharp crust-mantle transition. (b) Accepted waveforms matched to the velocity structures of (a). The dotted line illustrates the one standard deviation bounds of the receiver function stack.

(shown in Figure 8a) produced an adequate match to the data(Figure 8b). Many of the details of each velocity structure are lost in this presentation. However, the range of possible velocities at different depths is well represented. Near-surface P velocities vary between 5.08 and 5.82 km/sec. The largest range in velocities(approaching 0.96 km/sec) occurs near the depth 15 km, and Pn velocities vary between 7.65 and 8.10 km/sec(models with velocities higher than 8.20 km/sec were discarded). A detailed analysis of the velocity models identifies the common features in the waveforms, among them a strong near-surface velocity gradient, a slight-to-moderate decrease in velocity from approximately 8 to 15 km, and a sharp crust-mantle boundary at 30-32.5 km. No models indicate significant positive velocity gradients throughout the lower crust, all models show either approximately constant velocities or a decrease in velocity. Although this results is limited to around TJN site, the crustal thickness and velocity of the Moho are similar to the previous studies(Lee, 1979; Kim and Kim, 1983; Kim, 1995; Song, 2000).

We separate the solution models into two groups based on differences in the mid-crust: those models with roughly constant velocities(Figure 9a) and those models with a mid-crustal low-velocity zone(Figure 9b). Both groups of models contain similar lower-crustal structure. Note that the constant-velocity models have deeper moho discontinuity than the

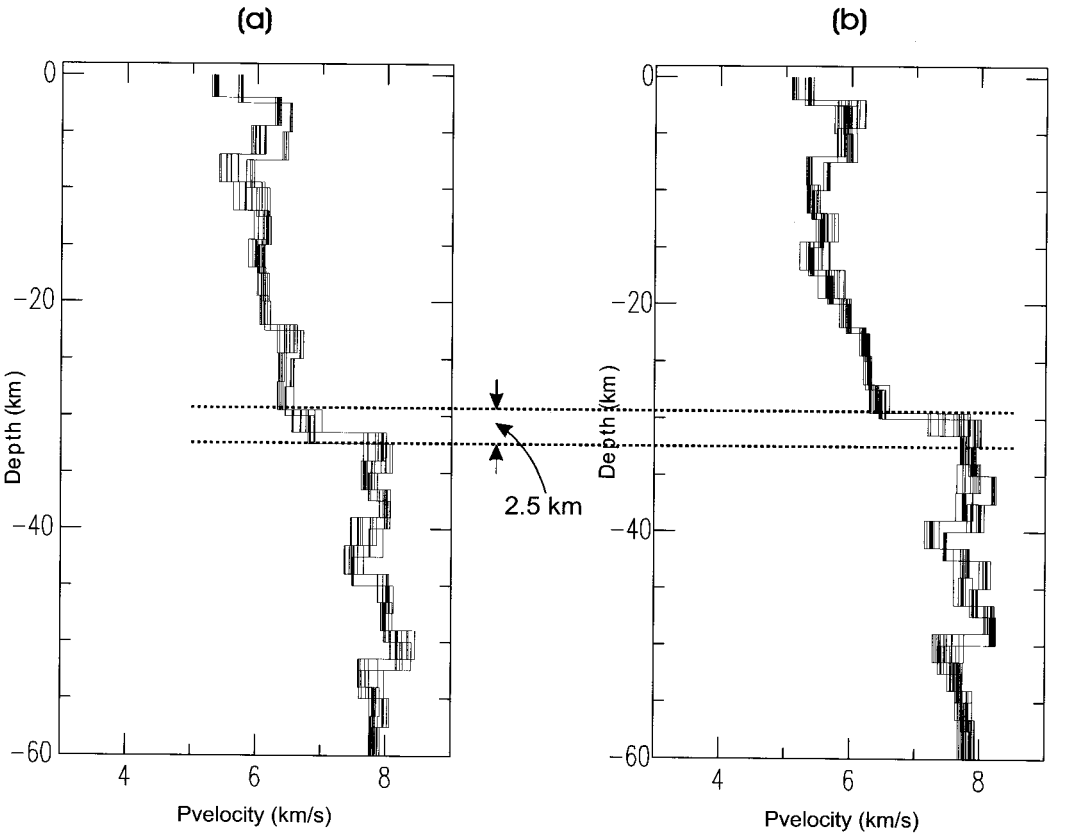

Fig. 9. Comparison of two groups of velocity structure from the TJN south receiver function. (a) The group of models with a mid-crust of nearly constant velocity. (b) The group of models with a slight low-velocity zone in the mid-crust. Note trade-off between the average wave velocity above the perturbation and the depth to the perturbation.

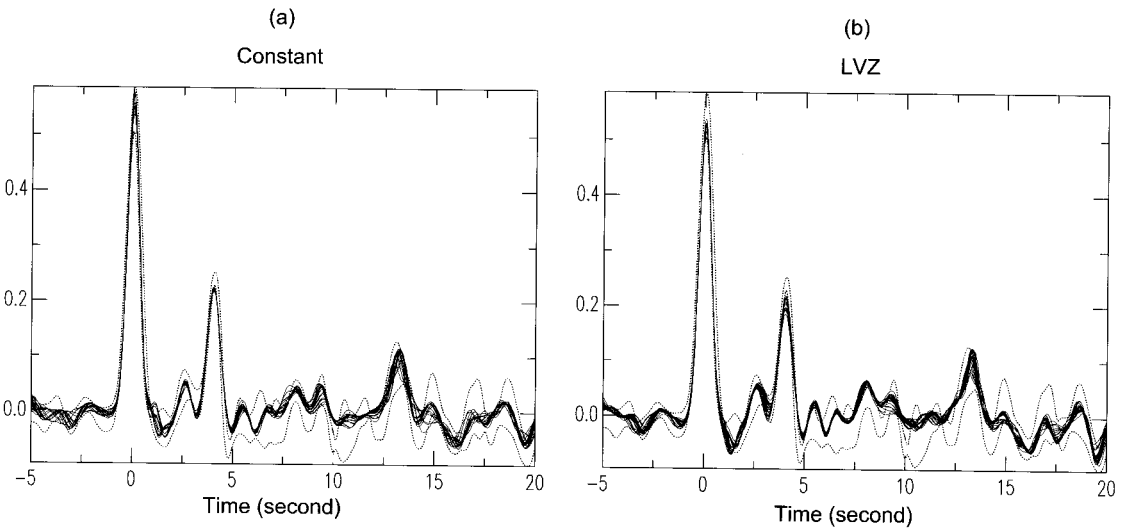

Fig. 10. The waveform fits corresponding to the group of nearly constant velocity structure (a) and the group of low velocity structure (b). The dotted lines represent one standard deviation bounds for the stacked receiver function.

low-velocity models by 2.5 km(Figure 9). The "low-velocity group" of mid-crust is very similar to Song's (2000) model in that the crustal thickness is about 33 km with average P-wave velocity of about 6.3 km/s overlying a mantle of Pn velocity near 7.9 km/sec. However, since the receiver function technique is sensitive to a depth-velocity ratio, not to the absolute velocity of the model, a substantial trade-off exists between the average wave velocity above the perturbation and the depth to the perturbation(Ammon *et al.*, 1990). Therefore, It is difficult to distinguish between the two velocity structures on the basis of receiver function waveforms alone(Figure 10).

So, in order to reduce the inherent nonuniqueness of the receiver function inversion modeling, addition of a priori information is necessary. Since the receiver functions are more sensitive to shear velocity, the combination of P wave receiver function and surface wave observations, both primarily sensitive to the shear wave velocity structure, could provide a more tightly constrained shear velocity estimate. Recently, it is reported that joint inversion of P wave receiver functions and surface wave phase velocities is very efficient to avoid over-interpretation of single data sets(Julia *et al.*, 2000). It is an avenue worth investigating in this area when the appropriate data exist or as a feasibility study prior to a data collection experiment.

5. Conclusion

To investigate the crustal structure under the Taejon(TJN) seismic station, a linearized time-domain inversion technique is applied to stacked teleseismic radial receiver function obtained from earthquakes in Indonesia. The main conclusions of this study can be summarized as follows:

1. Average crustal P-wave velocity lies between 5.8 and 6.3 km/sec, and crustal thickness and upper mantle P-wave velocity range from 30 to 32.5 km and from 7.75 to 7.95 km/sec, respectively.

2. The inversion indicates no velocity discontinuity or significant positive velocity gradient throughout the crust.

3. The inversion resulted in two groups based on difference in the mid-crust; one group of models with a low-velocity zone and the other group with nearly constant velocity.

4. Since the receiver function technique is sensitive to depth-velocity ratio, only additional a priori information can reduce the inherent nonuniqueness.

Acknowledgement

This study was supported by the BK 21 project of Seoul National University in part and also by the Korean Earthquake Engineering Research Center (KEERC) of Seoul National University in part. We thank Professors R. B. Herrmann at Saint Luois University and C. J. Ammon at Penn State University for providing computer programs and giving helpful comments throughout the study.

References

Ammon, C. J., 1991, The isolation of receiver effects from teleseismic P waveforms, Bulletin of Seismological Society of America, 81, 2504-2510.

Ammon, C. J., G. E. Randall and G. Zandt, 1990, On the non-uniqueness of receiver function inversions, Journal of Geophysical Research, 95, 15303-15318.

Ammon, C. J., G. Zandt, 1993, Receiver structure beneath the southern Mojave block California, Bulletin of Seismological Society of America, 83, 737-755.

Bath, M., and R. Stefansson, 1966, S-P conversions at the base of the crust, Annali Di Geofisica, 19, 119-130.

Clayton, R. W., and R. A. Wiggins, 1976, Source shape estimation and deconvolution of teleseismic bodywaves, Geophysical Journal of the Royal Astronomical Society, 47, 151-177.

Constable, S. C., R. L. Parker, and C. G. Constable, 1987, Occam's inversion: A practical algorithm for generating smooth models from electromagnetic sounding data, Geophysics, 52, 289-300.

Helmberger, D. V., and R. A. Wiggins, 1971, Upper mantle structure of the midwestern United States, Journal of Geophysical Research, 76, 3229-3245.

Julia, J., C. J. Ammon, R. B. Herrmann, A. M. Correig, 2000, Joint inversion of receiver function and surface wave dispersion observations, Geophysical Journal International, 143, 1-19.

Kim, S. K., 1995, A Study on the crustal structure of the Korean peninsula, Journal of the Geological Society of Korea, 31, 393-403 (in Korean).

Kim, S. J., and S. G. Kim, 1983, A Study on the crustal structure of south Korea by using seismic waves, The

Journal of the Korean Institute Mining Geology, 16, 51-61 (in Korean).

Kim, S. K., and B. H. Jung, 1985, Crustal structure of the southern part of Korea, The Journal of the Korean Institute of Mining Geology, 18, 151-157 (in Korean).

Langston, C. A., 1977, Corvallis, Oregon, crustal and upper mantle receiver structure from teleseismic P and S waves, Bulletin of Seismological Society of America, 67, 1029-1050.

Langston, C.A., 1979, Structure under Mount Rainier, Washington, inferred from teleseismic body waves, Journal of Geophysical Research, 84, 4749-4762.

Lee, K., 1979, On crustal structure of the Korean peninsula, Journal of the Geological Society of Korea, 15, 253-258.

Owens, T. J., 1984, Determination of crustal and upper mantle structure from analysis of broadband teleseismic P-waveforms, Ph. D. thesis, The University of Utah, Salt Lake City, UT.

Owens, T. J., G. Zandt, and S. R. Taylor, 1984, Seismic evidence for an ancient rift beneath the Cumberland plateau, Tennessee: A detailed analysis of broadband teleseismic P waveforms, Journal of Geophysical Research, 89, 7783-7795.

Owen, T. J., S. R. Taylor, and G. Zandt, 1987, Crustal structure at regional seismictest network stations determined from inversion of broadband teleseismic P waveforms, Bulletin of Seismological Society of America, 77, 631-662.

Song, S. G., 2000, A study on velocity structure of the Korean peninsula using earthquake data, M.S. thesis, The Seoul National University.

2001년 1월 22일 원고접수
2001년 3월 26일 원고채택